American Mineralogist, Volume 91, pages 551–559, 2006

The size distribution of exsolution lamellae in iron-free clinopyroxene

STEPHAN WEINBRUCH, VOLKER STYRSA, AND THOMAS DIRSCH*

Institut für Angewandte Geowissenschaften, Technische Universität Darmstadt, Schnittspahnstr. 9, D-64287 Darmstadt, Germany

ABSTRACT

The size distribution of pigeonite and diopside exsolution lamellae on "001," obtained at temperatures of 1100, 1200, and 1300 °C and annealing times between 2 and 4320 h, was studied by transmission electron microscopy. A total of 5192 pigeonite and 5286 diopside lamellae was studied. At all three temperatures, the size distributions of pigeonite and diopside lamellae are smaller during exsolution compared to the subsequent coarsening process. The final size distributions are time invariant, indicating that a steady-stage distribution is reached. The theory of Ardell (1972a), which assumes volume diffusion as rate-limiting process and takes into account the non-zero volume fraction of the precipitates, describes the experimental size distributions quite well and also leads to the observed exponent of three in the rate law.

Keywords: exsolution, clinopyroxene, size distribution, exsolution lamella, electron microscopy, experimental petrology, kinetics

INTRODUCTION

The wavelength of "001" exsolution lamellae [i.e., lamellae with composition planes approximately parallel to (001)] has been often used to constrain cooling rates of terrestrial and extraterrestrial rocks (e.g., Takeda et al. 1975; Grove 1982; Watanabe et al. 1985; Brizi and Mellini 1992; Weinbruch and Müller 1995; McCallum and O'Brien 1996; Weinbruch et al. 2001; Ferraris et al. 2002). The cooling rate estimates are based on coarsening of the exsolution lamellae observed during isothermal annealing (McCallister 1978; Nord and McCallister 1979; Weinbruch et al. 2003), or continuous cooling experiments (Grove 1982; Fukuda et al. 1987; Weinbruch et al. 2001).

In a recent study by Weinbruch et al. (2003), the exsolution mechanism and the coarsening kinetics in Fe-free clinopyroxene were investigated in detail. From the long-term isothermal annealing experiments (up to 4320 h), an exponent of approximately three was obtained in the rate law for coarsening (Weinbruch et al. 2003), indicating volume diffusion within both phases as rate-limiting process (e.g., Doherty 1983; Joesten 1991; Gleiter 1996). The grain-size distributions for coarsening of single-phase materials and for multiphase materials have been derived theoretically (see the excellent reviews by Martin and Doherty 1976; Ardell 1988; Joesten 1991; Gleiter 1996, and references therein). However, the experimental database is scanty for geomaterials (e.g., Eberl et al. 1990, 1998; Joesten 1991).

In the present study, we investigate the development of the size distribution of pigeonite and diopside "001" exsolution lamellae during coarsening and compare the results with predictions of various theoretical models. This paper complements our previous publication (Weinbruch et al. 2003) where the exsolution mechanism and coarsening kinetics were described.

* E-mail: dh6d@hrzpub.tu-darmstadt.de

EXPERIMENTAL METHODS

Isothermal annealing experiments were carried out with synthetic Fe-free clinopyroxene of composition $En_{45.1}Di_{54.9}$ at temperatures of 1100 °C (10 min to 4320 h), 1200 °C (1 h to 720 h), and 1300 °C (1 h to 360 h). The width of pigeonite and diopside "001" exsolution lamellae was determined by transmission electron microscopy (TEM). All experimental details can be found in our previous paper (Weinbruch et al. 2003).

RESULTS

The width of 30 to 480 pigeonite and diopside "001" exsolution lamellae was determined on each sample leading to a total of 5192 lamellae investigated for pigeonite, and 5286 lamellae for diopside. The exact locations, where the width of the individual lamellae was measured, was chosen randomly to avoid any bias in the data. The development of the microstructure during coarsening at a temperature of 1200 °C is illustrated in Figure 1 (additional TEM images of exsolution lamellae can be found in Weinbruch et al. 2003). The arithmetic mean and the standard deviation for the pigeonite and diopside lamellae width as function of temperature and annealing time are listed in Table 1. The ratio of the diopside/pigeonite lamellae width (Table 1) increases with increasing annealing temperature, and the following mean values were obtained: 1.63 for 1100 °C, 1.95 for 1200 °C, and 2.28 for 1300 °C. From these ratios, the volume fraction of the two phases can be determined (1100 °C: 62.0 vol% Di and 38.0 vol% Pig; 1200 °C: 66.1 vol% Di and 33.9 vol% Pig; 1300 °C: 69.8 vol% Di and 30.2 vol% Pig).

The size distributions of exsolution lamellae encountered at a temperature of 1100 °C are displayed in Figures 2 (pigeonite) and 3 (diopside) as function of annealing time. Shown is the reduced lamellae width ω', which is obtained by normalizing (separately for each temperature and annealing time) the measured lamellae width l to the mean value $\overline{l}$ ($\omega' = \frac{l}{\overline{l}}$). The size distribution of the reduced lamellae width is defined that $f'(\omega')d\omega'$ is the probability, normalized to unity, that a given lamella has a reduced

0003-004X/06/0004–551$05.00/DOI: 10.2138/am.2006.1944

TABLE 1. Width of "001" exsolution lamellae

Time (h)	Pigeonite		Diopside		Di/Pig*	Process†
	arithmetic mean ± standard deviation (nm); n‡					
1100 °C: λ_0 = 11.97 nm§; t_0 = 60 h						
12	4.53 ± 0.56	131	6.74 ± 1.44	151	1.49	exs.
18.5	4.60 ± 1.23	107	7.68 ± 1.88	107	1.67	exs.
24	5.02 ± 1.25	326	6.82 ± 1.72	347	1.36	exs.
48	4.93 ± 1.10	209	7.55 ± 2.49	217	1.53	exs.
72	5.15 ± 1.26	469	8.46 ± 2.30	480	1.64	coars.
96	9.16 ± 4.05	217	12.27 ± 4.22	222	1.34	coars.
120	7.98 ± 2.43	101	13.94 ± 3.29	102	1.75	coars.
360	15.54 ± 6.43	142	22.66 ± 7.13	140	1.46	coars.
720	14.67 ± 4.45	145	27.17 ± 6.91	143	1.85	coars.
1440	17.23 ± 6.64	194	33.52 ± 10.52	188	1.95	coars.
2160	20.09 ± 7.53	157	37.77 ± 11.17	146	1.88	coars.
4320	29.45 ± 12.94	178	48.86 ± 18.50	171	1.66	coars.
1200 °C: λ_0 = 17.91 nm§; t_0 = 18 h						
8	5.88 ± 1.28	157	11.01 ± 2.34	164	1.87	exs.
12	6.19 ± 1.39	178	12.73 ± 4.70	197	2.06	exs.
24	7.90 ± 1.69	166	14.97 ± 3.02	170	1.89	coars.
48	8.14 ± 2.15	92	18.87 ± 4.66	93	2.32	coars.
72	12.68 ± 3.85	155	26.55 ± 8.58	152	2.09	coars.
96	14.11 ± 5.39	166	28.19 ± 8.20	168	2.00	coars.
120	12.86 ± 4.41	241	26.59 ± 8.05	246	2.07	coars.
120	11.04 ± 4.35	189	20.99 ± 7.81	188	1.90	coars.
240	18.99 ± 8.08	137	34.65 ± 12.44	134	1.82	coars.
360	28.94 ± 11.68	106	54.62 ± 17.87	103	1.89	coars.
360	29.58 ± 12.08	31	44.46 ± 13. 65	30	1.50	coars.
720	32.04 ± 11.17	102	63.49 ± 19.00	104	1.98	coars.
1300 °C: λ_0 = 21.15 nm§; t_0 = 8 h						
2	8.33 ± 1.56	87	11.24 ± 2.59	85	1.35	exs.
3	7.32 ± 1.25	218	15.04 ± 3.91	227	2.05	exs.
4	7.43 ± 1.61	130	14.09 ± 4.53	138	1.90	exs.
12	11.56 ± 5.22	135	22.57 ± 7.54	144	1.95	coars.
24	12.70 ± 2.67	101	40.22 ± 9.66	101	3.17	coars.
72	22.07 ± 11.78	174	50.36 ± 22.72	176	2.28	coars.
120	21.17 ± 5.15	130	61.48 ± 24.28	138	2.90	coars.
360	33.70 ± 9.71	121	88.62 ± 30.00	114	2.63	coars.

* Ratio of diopside/pigeonite exsolution lamellae width.
† exs. = exsolution, coars. = coarsening.
‡ Number of lamellae measured.
§ Based on arithmetic mean.

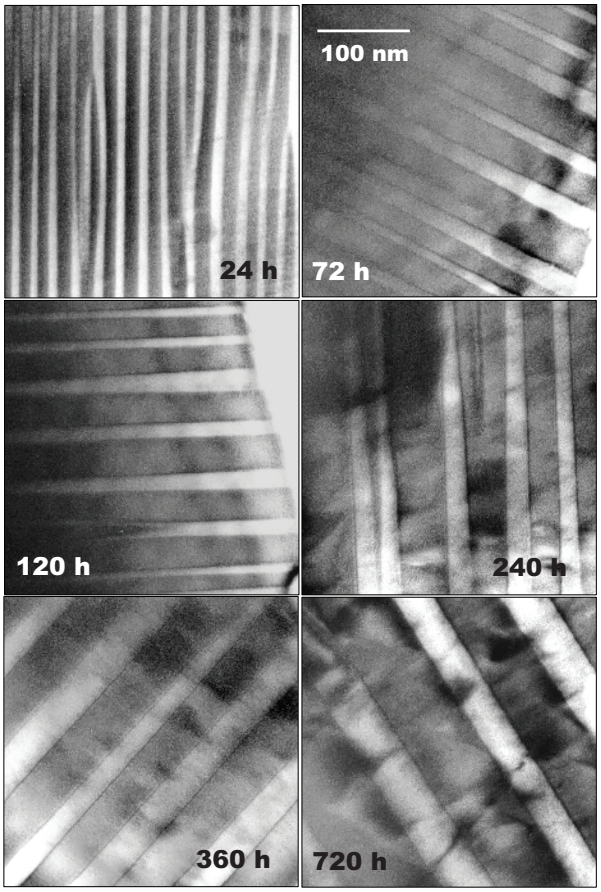

FIGURE 1. TEM bright-field images of coarsened exsolution lamellae on "001" in Fe-free clinopyroxene (1200 °C). Bright lamellae are pigeonite; dark lamellae are diopside.

width in the size interval between ω' and ω' + dω'. This function is independent of time, although the value of $\overline{l}$ increases with time. Parameters of the size distributions of the reduced lamellae width (1st and 9th decile, interdecile range, standard deviation) are given in Table 2. At all three temperatures investigated, the size distributions of pigeonite lamellae are smaller during exsolution compared to the subsequent coarsening (Fig. 2). For diopside lamellae, this effect is less pronounced (Fig. 3).

To compare the empirical size distributions with the predictions of theoretical models, it is necessary to demonstrate that a steady-stage distribution, where the size distribution of the reduced lamellae width remains invariant with time, is reached during the experiments. For this purpose, the experimental results of all temperatures are grouped together (separately for pigeonite and diopside) and four different situations were distinguished. First, all samples where exsolution was observed but coarsening has not yet taken place are shown (Figs. 4a and 4e). Criteria to define the boundary between exsolution and coarsening include the width of the "001" lamellae, the presence of "100" lamellae, and the smoothness of the phase boundary between pigeonite and diopside (for details see Weinbruch et al. 2003). Samples with coarsened exsolution lamellae can be grouped according to their mean lamellae width $\overline{l}$ which is compared to $\overline{l}_0$, the mean value prior to coarsening. Three different groups were defined: $\overline{l}_0 < \overline{l} \le 2 \times \overline{l}_0$ (Figs. 4b and 4f), $2 \times \overline{l}_0 < \overline{l} \le 4 \times \overline{l}_0$ (Figs. 4c and 4g), and $4 \times \overline{l}_0 < \overline{l}$ (Figs. 4d and 4h). The size distributions of the reduced lamellae width of the last two groups are almost identical (for pigeonite and diopside, each), clearly demonstrating that the steady-stage distribution is reached. In principle, it could be suspected that grouping together results from different temperatures is not appropriate, as the volume fraction of the two exsolved phases (which affects the size distribution) is temperature dependent. However, the effect of volume fraction on the size distribution is most pronounced at small values below 0.2 (e.g., Ardell 1972a) and, thus, can be neglected for the high-volume fractions observed in our experiments.

Coarsening of the "001" exsolution lamellae can be described by the following empirical equation (e.g., Carpenter 1991):

$$\lambda_t^n - \lambda_0^n = n * k * \exp(-\Delta H / RT) * (t - t_0) \quad (1)$$

with λ_t the average wavelength at time t, λ_0 the average wavelength at time t_0, ΔH an activation energy, R the gas constant, T the temperature (K), and n and k empirical constants. In our previous

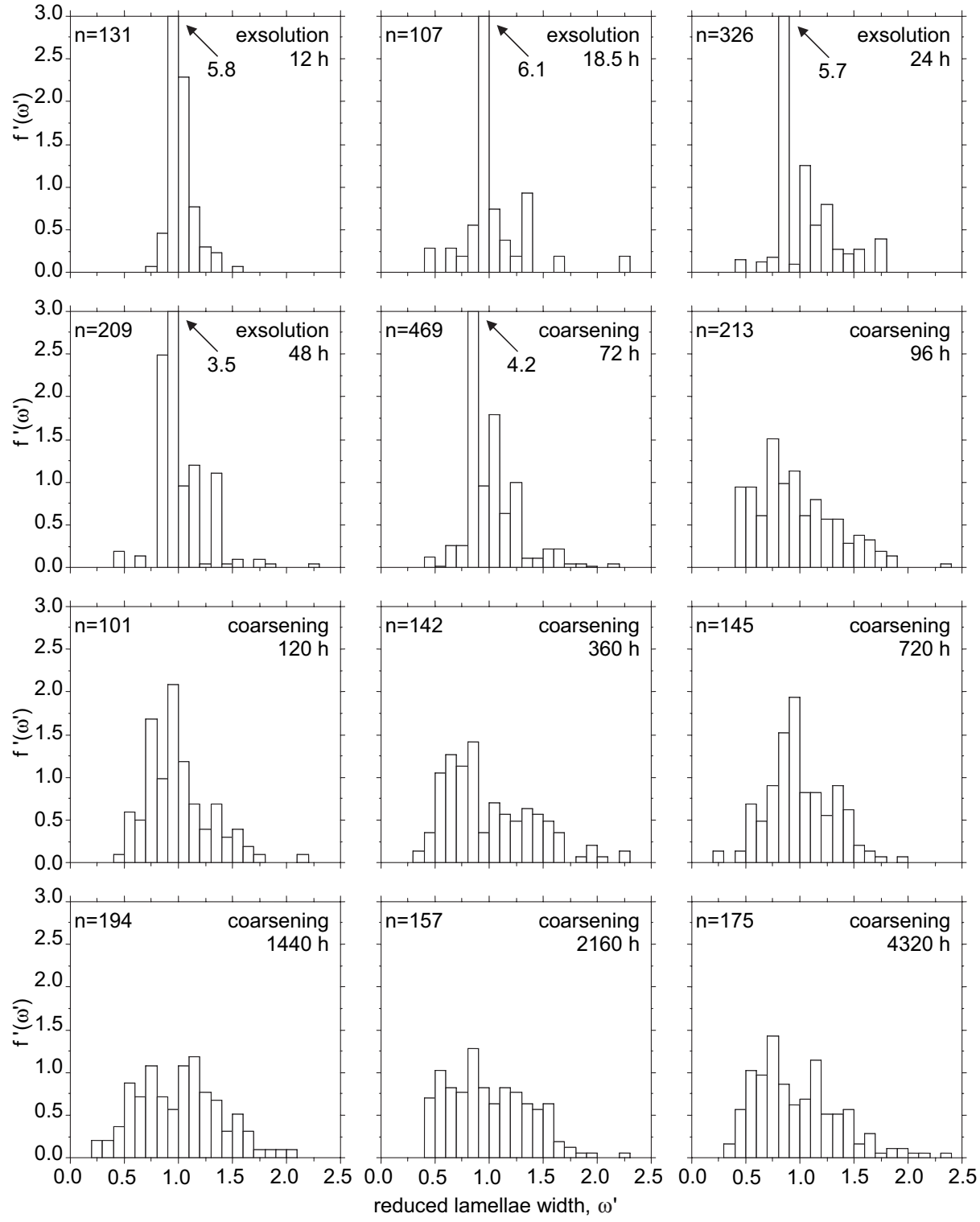

FIGURE 2. Development of the size distribution of pigeonite lamellae with time at a temperature of 1100 °C.

paper (Weinbruch et al. 2003), the median of the wavelength was fitted to Equation 1 to obtain a robust (i.e., independent of outliers) estimate for n, k, and ΔH. However, as the arithmetic mean of the wavelength is used in all theoretical treatments of coarsening, we have decided to use this parameter (instead of the median) in the present paper. Based on the arithmetic mean

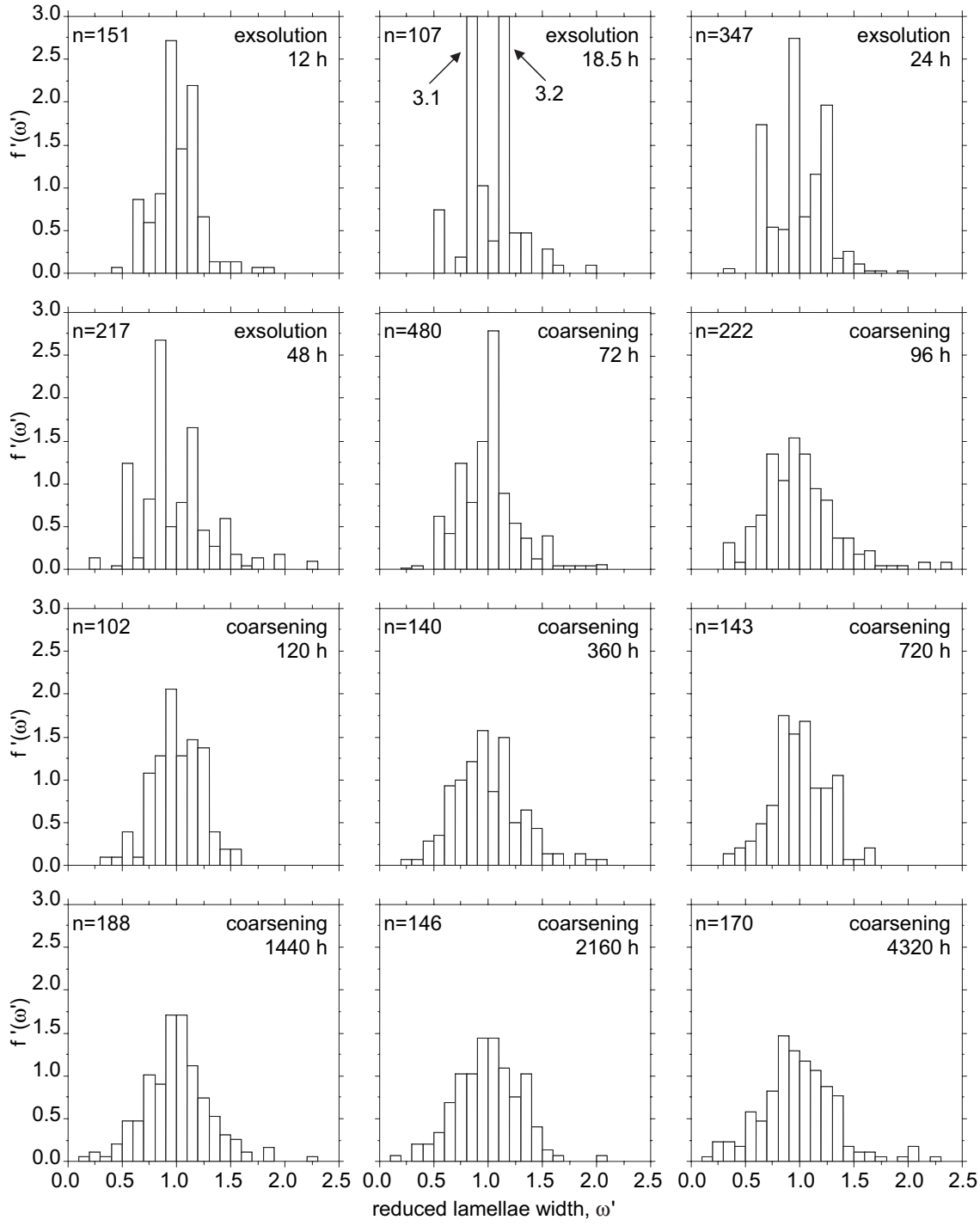

FIGURE 3. Development of the size distribution of diopside lamellae with time at a temperature of 1100 °C.

(Table 1), somewhat different values (compared to Weinbruch et al. 2003) are obtained from the multiple regression analysis: $n = 2.97$; $k = 6.07 \times 10^{14}$ [nm$^{2.97}$/h]; $\Delta H = 83.2$ [kcal/mol]. Most important is the fact that the exponent n is still closer to 3, in comparison to the estimate based on the median of the wavelength ($n = 2.87$).

DISCUSSION

Coarsening kinetics

Microstructural changes stimulated by reduction of the interfacial energy (in the absence of external potential fields) may be divided into three different categories (Gleiter 1996):

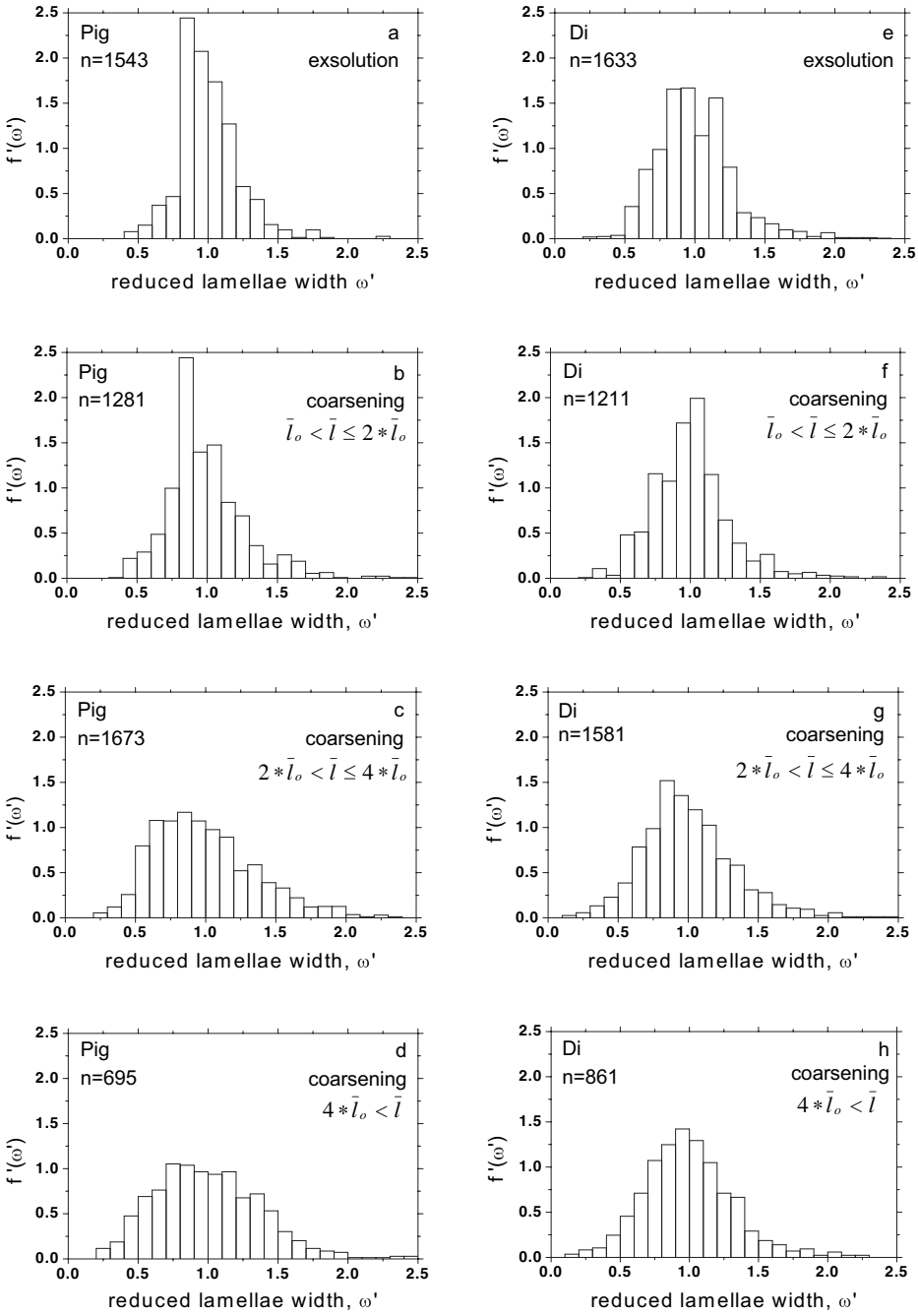

FIGURE 4. Observed size distributions for pigeonite (Pig) and diopside (Di) during exsolution and coarsening. The different coarsening regimes are distinguished by the increasing mean value of the lamellae width (see text for details).

microstructural changes in single-phase materials (domain and grain growth); microstructural changes in polyphase materials with dispersion structure (Ostwald ripening); and microstructural changes in polyphase materials with duplex structure. A duplex structure is defined in this context as an oriented crystallographic unit consisting of two phases with a definite orientation relationship. However, it should be emphasized here that the processes involved in the microstructural changes of duplex structures are identical to Ostwald ripening (Cline 1971; Ardell 1972b).

For Ostwald ripening, the change of the linear dimension d of any microstructural feature with time t is scaled by the following equation (Herring 1950):

$$d^n = d_0^n + \alpha G t \tag{2}$$

with d_0 the value of d at $t = 0$, n the scaling exponent, G the parameter of the appropriate mass transport process, and α a dimensionless parameter.

TABLE 2. Parameters of the size distribution of the reduced lamellae width

Time (h)	Pigeonite				Diopside				Process*
	d_1†	d_9†	d_9-d_1	st.dev.‡	d_1†	d_9†	d_9-d_1	st.dev. ‡	
1100 °C									
12	0.94	1.17	0.23	0.12	0.73	1.26	0.53	0.21	exs.
18.5	0.86	1.38	0.52	0.27	0.83	1.29	0.46	0.24	exs.
24	0.86	1.30	0.44	0.25	0.64	1.28	0.64	0.25	exs.
48	0.87	1.31	0.44	0.22	0.59	1.42	0.83	0.33	exs.
72	0.84	1.28	0.44	0.25	0.69	1.36	0.67	0.27	coars.
96	0.56	1.56	1.00	0.44	0.63	1.44	0.81	0.34	coars.
120	0.66	1.41	0.75	0.30	0.72	1.28	0.56	0.24	coars.
360	0.57	1.53	0.96	0.41	0.66	1.40	0.74	0.31	coars.
720	0.63	1.41	0.78	0.30	0.67	1.32	0.65	0.25	coars.
1440	0.50	1.50	1.00	0.39	0.63	1.38	0.75	0.31	coars.
2160	0.54	1.50	0.96	0.37	0.66	1.38	0.72	0.30	coars.
4320	0.54	1.54	1.00	0.44	0.54	1.37	0.83	0.38	coars.
1200 °C									
8	0.72	1.27	0.55	0.22	0.77	1.16	0.39	0.21	exs.
12	0.70	1.29	0.59	0.22	0.68	1.48	0.80	0.37	exs.
24	0.71	1.28	0.57	0.21	0.77	1.23	0.46	0.20	coars.
48	0.76	1.43	0.67	0.26	0.68	1.32	0.64	0.25	coars.
72	0.67	1.37	0.70	0.30	0.70	1.31	0.61	0.32	coars.
96	0.60	1.50	0.90	0.38	0.64	1.36	0.72	0.29	coars.
120	0.63	1.50	0.87	0.34	0.67	1.37	0.70	0.30	coars.
120	0.59	1.57	0.98	0.39	0.62	1.53	0.91	0.37	coars.
240	0.52	1.65	1.13	0.43	0.57	1.50	0.93	0.36	coars.
360	0.52	1.50	0.98	0.40	0.63	1.34	0.71	0.33	coars.
360	0.54	1.43	0.89	0.41	0.68	1.40	0.72	0.31	coars.
720	0.59	1.44	0.85	0.35	0.62	1.34	0.72	0.30	coars.
1300 °C									
2	0.78	1.22	0.44	0.19	0.77	1.21	0.44	0.23	exs.
3	0.83	1.19	0.36	0.17	0.75	1.33	0.58	0.26	exs.
4	0.75	1.17	0.42	0.22	0.65	1.38	0.73	0.32	exs.
12	0.67	1.35	0.68	0.45	0.66	1.44	0.78	0.33	coars.
24	0.75	1.24	0.49	0.21	0.72	1.31	0.59	0.24	coars.
72	0.55	1.55	1.00	0.53	0.52	1.59	1.07	0.45	coars.
120	0.42	1.31	0.89	0.24	0.42	1.49	1.07	0.39	coars.
360	0.64	1.34	0.70	0.29	0.63	1.48	0.85	0.34	coars.

* exs. = exsolution, coars. = coarsening.
† d_1 = first decile, d_9 = ninth decile.
‡ Standard deviation.

Equation 2 describes coarsening after termination of the reaction that leads to formation of the microstructure (e.g., exsolution). Alternatively, the time t in Equation 2 may be substituted by the term $(t - t_0)$, with t_0 the time to complete the reaction, as is the case in the empirical Equation 1.

The scaling exponent n varies for different rate-controlling processes: $n = 2$ for interface-limited growth (Doherty 1982); $n = 3$ for volume diffusion (Wagner 1961; Lifshitz and Slyozov 1961; Doherty 1982); $n = 4$ for grain-boundary diffusion (Ardell 1972b; Kirchner 1971); and $n = 5$ for dislocation-pipe diffusion (Ardell 1972b). The appropriate expressions for α and G can be found in Gleiter (1996).

For coarsening of lamellar (duplex) structures, two different mechanisms have been proposed. According to Cline (1971) and Graham and Kraft (1966), the curvature at the termination of a lamella induces a flux of atoms from the lamella to the matrix leading to a recession of the termination and, therefore, to coarsening. According to Brady (1987), this mechanism yields the following rate law for coarsening of exsolution lamellae:

$$\lambda^2 = \lambda_0^2 + kt \tag{3}$$

with λ the wavelength at time t, λ_0 the wavelength at $t = 0$, and k an empirical constant. As we have observed an exponent of 3 (within error limits), the rate law of Brady (1987) is not supported by our experimental data. It should be emphasized here that we determined the exponent directly by fitting the experimental data to Equation 1. In contrast, the exponent was imposed by most previous workers, as they have used equations with a constant value (of either three or two). An exponent of 3 was also reported in many empirical studies of coarsening of plate-like precipitates (see Doherty 1982, and references therein).

The second model for coarsening of duplex structures assumes diffusion from finely spaced to widely spaced lamellae that are separated by a migrating boundary (Livingston and Cahn 1974). A sharp boundary between regions of finely and widely spaced lamellae was observed in aligned eutectoids (e.g., Livingston and Cahn 1974), but not for exsolution textures, neither in the present study nor in previous literature. Therefore, the mechanism advocated by Livingston and Cahn (1974) can be excluded in our case.

Size distribution of the exsolution lamellae

The size distribution of coarsened precipitates has found wide attention in material science (see the reviews by Martin and Doherty 1976; Ardell 1988; Gleiter 1996). However, it appears that there are still substantial discrepancies between modern theories and the experimental database. According to Ardell (1988), no single theory accurately describes all the data of any given alloy system.

In the following, the empirical size distributions of "001" exsolution lamellae of pigeonite and diopside are compared to the predictions of various theoretical treatments. To warrant that a steady-stage distribution is reached, only samples with a mean lamellae width $\overline{l}$ larger than four times the initial lamellae width $\overline{l}_0$ are included in this comparison. The resulting empirical size distributions (Figs. 4d and 4h) include 695 lamellae for pigeonite (1100 °C: 2160 h, 4320 h; 1200 °C: 360 h, 720 h; 1300 °C: 360 h) and 861 lamellae for diopside (1100 °C: 1440 h, 2160 h, 4320 h; 1200 °C: 720 h; 1300 °C: 120 h, 360 h).

Theoretical grain-size distributions $f(\rho)$ are generally derived for the particle radius r normalized to the critical radius r^* ($\rho = r/r^*$). The critical radius r^* is the equilibrium radius of a precipitate (i.e., the particle does neither grow nor shrink). To facilitate comparison to experimental size distributions, the theoretical distributions can be described in terms of the reduced particle radius $\rho = r/r'$ (with r' the mean value of the particle radius), because r^* is generally unknown. The distribution function for the reduced particle radius $f'(\rho')$ is then given by:

$$f'(\rho') = \overline{\rho} f(\rho) \tag{4}$$

for a precipitate volume fraction φ of zero, ρ' is one and, thus, $f'(\rho') = f(\rho)$ (e.g., Ardell 1972a).

The observed grain-size distributions will first be compared to the predictions of the LSW theory (Lifshitz and Slyozov 1961; Wagner 1961) for Ostwald ripening and volume diffusion, grain boundary diffusion and interface reactions as rate-limiting process. Derivation of the different size distribution functions is beyond the scope of the present paper and can be found in the original papers cited below. The theoretical grain-size distribution functions are all scaled so that $\int_{\rho'=0}^{\rho'=\rho_{max}} f'(\rho')d\rho' = 1$.

According to the LSW theory (Lifshitz and Slyozov 1961; Wagner 1961), the grain-size distribution function for Ostwald ripening controlled by volume diffusion is given by:

$$f'(\rho') = \frac{4\rho'^2}{9}\left(\frac{3}{3+\rho'}\right)^{7/3}\left(\frac{3}{3-2\rho'}\right)^{11/3}\exp\left(\frac{-2\rho'}{3-2\rho'}\right) \text{ for } \rho' \le 3/2$$

and (5)

$$f'(\rho') = 0 \text{ for } \rho' > 3/2$$

For grain boundary diffusion as rate-controlling process, the LSW theory yields the following equation (Kirchner 1971; Ardell 1972b):

$$f'(\rho') = \frac{k\rho'^3 \exp\left(\frac{1}{2} - \left(\frac{2}{3(4/3-\rho')}\right) - \frac{1}{6\sqrt{2}}\left(\tan^{-1}\left(\frac{1+3\rho'/4}{\sqrt{2}}\right) - \tan^{-1}\left(\frac{1}{\sqrt{2}}\right)\right)\right)}{\left(1-\frac{3\rho'}{4}\right)^{19/6}\left(\frac{3\rho'^2}{16}+\frac{\rho'}{2}+1\right)^{23/12}} \quad (6)$$

for $\rho' \le 4/3$

and

$$f'(\rho') = 0 \text{ for } \rho' > 4/3.$$

The scaling factor k in Equation 6 is reported to be equal to 3/4 by Joesten (1991) and $(3/4)^4$ by Ardell (1972b). However, both values do not scale the integral of the grain-size distribution function to one (the appropriate value for k in Equation 6 was empirically found to be ≈ 0.63).

For interface-limited growth, the following grain-size distribution function was derived (Wagner 1961):

$$f'(\rho') = \frac{3\rho'}{4}\left(\frac{2}{2-\rho'}\right)^5\exp\left(\frac{-3\rho'}{2-\rho'}\right) \text{ for } \rho' \le 2$$

and (7)

$$f'(\rho') = 0, \text{ for } \rho' > 2.$$

The predictions of the LSW theory are compared to the empirical steady-stage size distributions of pigeonite (Fig. 5a) and diopside (Fig. 5b) exsolution lamellae on "001". The experimental distributions displayed in Figure 5 are identical to those of Figures 4d and 4h (i.e., we have plotted only data from long annealing times were $\overline{l} > 4 \times \overline{l}_0$). For volume diffusion and grain-boundary diffusion as rate-limiting processes, large deviations between theory and the experimental data are observed. Both the maximum of the size distribution function and the maximum value for the reduced lamellae width are not predicted accurately. For coarsening controlled by the kinetics of interface reactions, a broader size distribution is obtained, which is closer to the experimental distribution. However, this mechanism can still be ruled out, as it should lead to a parabolic rate law for the coarsening kinetics, which is in contradiction to the cubic rate law observed in our study.

The theory of diffusion-controlled particle coarsening developed by Lifshitz and Slyozov (1961) and Wagner (1961) was modified by Ardell (1972a) to take into account the volume fraction φ of the precipitates (this approach is generally referred to as modified LSW or MLSW theory). In the original LSW theory, it is assumed that the volume fraction of the precipitates is close to zero, which is often not the case. According to the theoretical treatment of Ardell (1972a), the exponent of three in the rate law is retained but the coarsening rate is increased. The size distribution becomes more symmetrical and broader compared to the original LSW theory. The theoretical size distribution can be calculated as follows:

$$f(\rho) = \frac{-3\rho^2}{d\rho^3/d\tau}\exp\left(\int_0^\rho \frac{3\rho^2 d\rho}{d\rho^3/d\tau}\right) \quad (8)$$

and

$$\frac{d\rho^3}{d\tau} = (\rho-1)(1+\beta\rho)\upsilon - \rho^3 \quad (9)$$

with r the particle radius, r^* the critical particle radius, $\rho = r/r^*$, $\tau = \ln(r^3)$ and β and υ parameters that depend on the volume fraction φ.

Equation 8 can be integrated analytically only when $\varphi = 0$ or $\varphi = 1$. For a volume fraction of zero, the results of the LSW theory are obtained. For a volume fraction of 1, the resulting particle size distribution function is formally identical to the distribution functions derived by Wagner (1961) for interface-controlled coarsening. The values for β, υ, and ρbar as functions of the volume fraction φ are listed in Ardell (1972a). The resulting grain-size distributions (based on the reduced particle radius) for volume fractions of 0.35 and 0.65 are displayed in Figures 5c and 5d. Equation 4 was used to convert the size distribution function based on the critical particle radius to the size distribution function based on the reduced particle radius. The MLSW theory of Ardell (1972a) fits the experimental data much better than the original LSW theory (Figs. 5c and 5d). It should also be noted here that the theoretical size distributions for volume fractions of 0.35 and 0.65 are almost identical.

The influence of volume fraction on coarsening has found wide attention in material science, and a rather large number of theories has been published since the classic paper of Ardell (1972a). As it is impossible to discuss all these theories in detail here, a few general remarks will be given in the following (the reader is referred to the review by Ardell 1988). All theoretical approaches to the influence of the precipitate volume fraction yield an exponent of three in the rate law. In addition, a broader size distribution than predicted by the LSW theory is obtained. The range of size distributions predicted by the different theoretical approaches, which take into account the effect of a non-zero volume fraction, is also shown in Figures 5c and 5d as a shaded area (for a volume fraction of $\varphi = 0.35$). As our experimental data are not better fitted by these theories, it is concluded that the effects of a non-zero volume fraction on the size distribution of the exsolution lamellae are sufficiently described by the MLSW theory of Ardell (1972a).

Related to a non-zero volume fraction is the problem of particle collisions (encounters) during growth. This effect was addressed explicitly by Davies et al. (1980). However, as coarsening of exsolution lamellae takes place by the retreat of lamellae terminations (Cline 1971; Brady 1987), encounters cannot occur in this process. Therefore, the theory of Davies et al. (1980) is not considered further. However, it should be noted here that the grain-size distribution obtained from the theory of Davies et al. (1980) also lies in the range of the different theories shown by

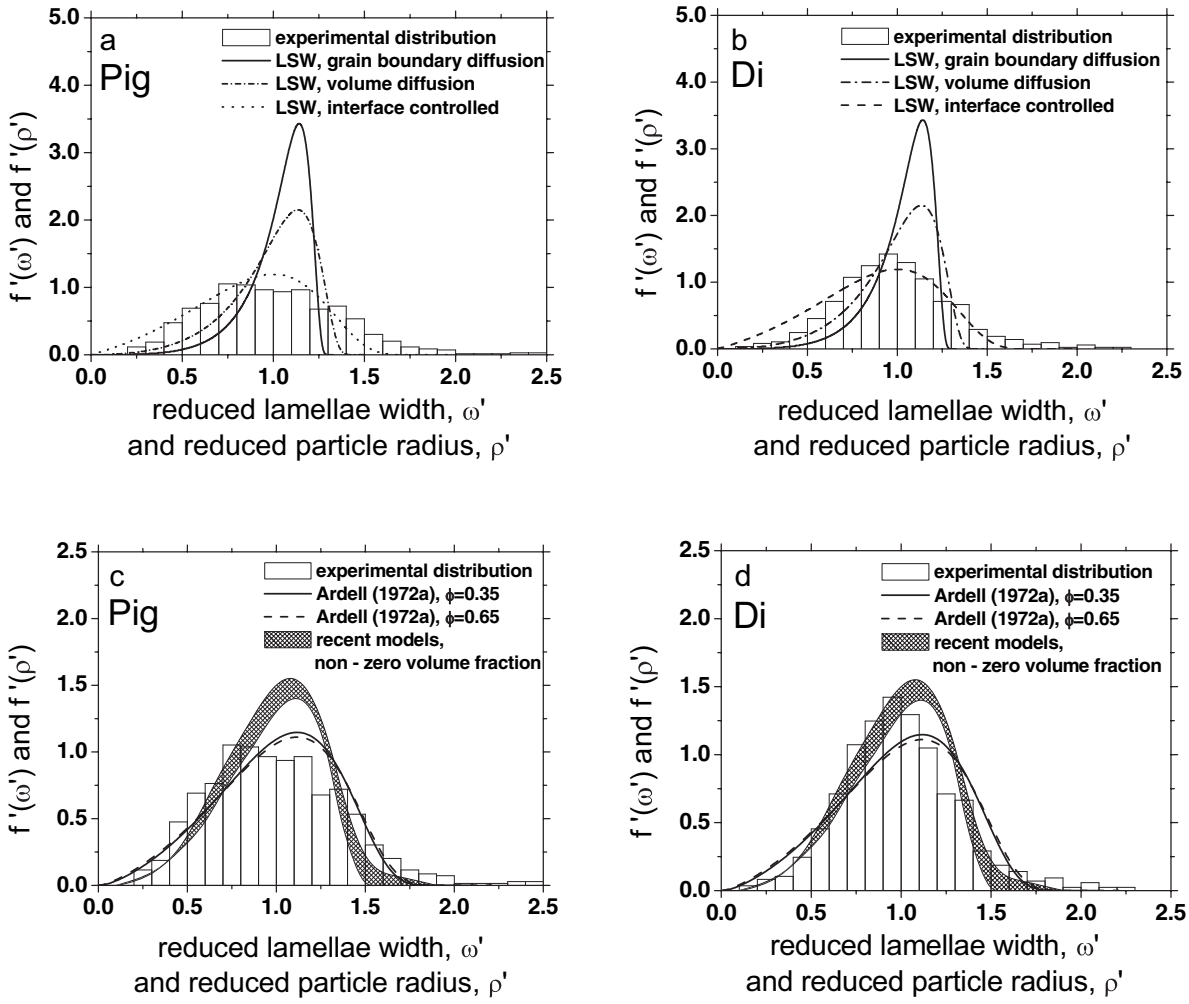

FIGURE 5. Comparison of experimental steady stage size distributions with the predictions of the LSW theory and volume diffusion, grain-boundary diffusion, and interface reactions as rate-limiting process (**a** and **b**) and various theories that take into account the effect of volume fraction (**c** and **d**). For the experimental data, the size distribution $f'(\omega')$ of the reduced lamellae width ω' is shown. The theoretical models predict the size distribution $f'(\rho')$ of spherical particles with the reduced particle radius ρ'.

the shaded area in Figures 5c and 5d.

The retreat of lamellae terminations as the mechanism for the coarsening process was discussed in detail by Brady (1987). Based on earlier work by Graham and Kraft (1966) and Cline (1971), a coarsening model for exsolution lamellae was developed that predicts a parabolic rate law. However, the parabolic rate law is not supported by our experimental data. The size distribution of exsolution lamellae was not addressed by Brady (1987). The preceeding work of Cline (1971), who considered the coarsening of rod-shaped composite structures, yielded a steady-stage distribution identical to the predictions of the classic LSW theory.

In conclusion, assuming volume diffusion as the rate-controlling process and taking into account the non-zero volume fraction of the exsolution lamellae leads to a reasonable agreement between theory and the experimental data. Although not developed for lamellar geometry, the theory of Ardell (1972a) can be used to describe the experimental size distributions of pigeonite and diopside exsolution lamellae on "001."

ACKNOWLEDGMENTS

We have benefited greatly from discussions with Peter van Aken and Wolfgang F. Müller. Financial support by the Deutsche Forschungsgemeinschaft is gratefully acknowledged. We would like to thank R.H. McCallister, K. Moore, and M. Tribaudino for constructive reviews.

REFERENCES CITED

Ardell, A.J. (1972a) The effect of volume fraction on particle coarsening: Theoretical considerations. Acta Metallurgica, 20, 61–71.

——— (1972b) On the coarsening of grain boundary precipitates. Acta Metallurgica, 20, 601–609.

——— (1988) Precipitate coarsening in solids: modern theories, chronic disagreement with experiment. In G.W. Lorimer, Ed., Phase Transformations '87, p. 485–494. Institute for Metals, London.

Brady, J.B. (1987) Coarsening of fine-scale exsolution lamellae. American Mineralogist, 72, 697–706.

Brizi, E. and Mellini, M. (1992) Kinetical modelling of exsolution textures in igneous pyroxenes. Acta Vulcanologica, 2, 87–93.

Carpenter, M.A. (1991) Mechanisms and kinetics of Al-Si ordering in anorthite: I. Incommensurate structure and domain coarsening. American Mineralogist, 76, 1110–1119.

Cline, H.E. (1971) Shape instabilities of eutectic composites at elevated temperatures. Acta Metallurgica, 19, 481–490.

Davies, C.K.L., Nash, P., and Stevens, R.N. (1980) The effect of volume fraction of precipitate on Ostwald ripening. Acta Metallurgica, 28, 179–189.

Doherty, R.D. (1982) Role of interfaces in kinetics of internal shape changes. Metal Science, 16, 1–13.

——— (1983) Diffusive phase transformations in the solid state. In R.W. Cahn and P. Haasen, Eds., Physical Metallurgy, 3rd edition, p. 933–1030. Elsevier, Amsterdam.

Eberl, D.D., Srodoń, J., Kralik, M., Taylor, B.E., and Peterman, Z.E. (1990) Ostwald ripening of clays and metamorphic minerals. Science, 248, 474–477.

Eberl, D.D., Drits, V.A., and Srodon, J. (1998) Deducing growth mechanisms for minerals from the shapes of crystal size distributions. American Journal of Science, 298, 499–533.

Ferraris, C., Folco, L., and Mellini, M. (2002) Chondrule thermal history from unequilibrated H chondrites: a transmission and analytical electron microscopy study. Meteoritics and Planetary Science, 37, 1299–1321.

Fukuda, K., Yamanaka, T., and Tokonami, M. (1987) Dependence of exsolution textures in synthetic augite on its composition and cooling rate. Mineralogical Journal, 13, 376–389.

Gleiter, H. (1996) Microstructure. In R.W. Cahn and P. Haasen, Eds., Physical Metallurgy, 4th edition, p. 843–942. Elsevier, Amsterdam.

Graham, L.D. and Kraft, R.W. (1966) Coarsening of eutectic microstructures at elevated temperatures. Transactions of the Metallurgical Society of AIME, 236, 94–102.

Grove, T.L. (1982) Use of exsolution lamellae in lunar clinopyroxenes as cooling rate speedometers: an experimental calibration. American Mineralogist 67, 251–268.

Herring, C. (1950) Effect of change of scale on sintering phenomena. Journal of Applied Physics, 21, 301–303.

Joesten, R.L. (1991) Kinetics of coarsening and diffusion-controlled mineral growth. In C.D.M. Kerrick, Ed., Contact Metamorphism, 26, p. 507–582. Reviews in Mineralogy, Mineralogical Society of America, Chantilly, Virginia.

Kirchner, H.O.K. (1971) Coarsening of grain-boundary precipitates. Metallurgical Transactions, 2, 2861–2864.

Lifshitz, I.M. and Slyozov, V.V. (1961) The kinetics of precipitation from supersaturated solid solutions. Journal of Physics and Chemistry of Solids, 19, 35–50.

Livingston, J.D. and Cahn, J.W. (1974) Discontinuous coarsening of aligned eutectoids. Acta Metallurgica, 22, 495–503.

Martin, J.W. and Doherty, R.D. (1976) Stability of microstructure in metallic systems, 298 p. Cambridge University Press, U.K.

McCallister, R.H. (1978) The coarsening kinetics associated with exsolution in an iron-free clinopyroxene. Contributions to Mineralogy and Petrology, 65, 327–331.

McCallum, I.S. and O'Brien, H.E. (1996) Stratigraphy of the lunar highland crust: Depths of burial of lunar samples from cooling-rate studies. American Mineralogist, 81, 1166–1175.

Nord, G.L. and McCallister, R.H. (1979) Kinetics and mechanisms of decomposition in $Wo_{25}En_{31}Fs_{44}$ clinopyroxene. Geological Society of America, Abstracts with program, 11, 488.

Takeda, H., Miyamoto, M., Ishii, T., and Lofgren, G.E. (1975) Relative cooling rates of mare basalts at the Apollo 12 and 15 sites as estimated from pyroxene exsolution data. Proceedings of the 6th Lunar Planetary Science Conference, 987–996.

Wagner, C. (1961) Theorie der Alterung von Niederschlägen durch Umlösen (Ostwald-Reifung). Zeitschrift für Elektrochemie, 65, 581–591.

Watanabe, S., Kitamura, M., and Morimoto, N. (1985) A transmission electron microscope study of pyroxene chondrules in equilibrated L-group chondrites. Earth and Planetary Science Letters, 72, 87–98.

Weinbruch, S. and Müller, W.F. (1995) Constraints on the cooling rates of chondrules from the microstructure of clinopyroxene and plagioclase. Geochimica et Cosmochimica Acta, 59, 3221–3230.

Weinbruch, S., Müller, W.F., and Hewins, R.H. (2001) A transmission electron microscope study of exsolution and coarsening in iron-bearing clinopyroxene from synthetic analogues of chondrules. Meteoritics and Planetary Science, 36, 1237–1248.

Weinbruch, S., Styrsa, V., and Müller, W.F. (2003) Exsolution and coarsening in iron-free clinopyroxene during isothermal annealing. Geochimica et Cosmochimica Acta, 67, 5071–5082.

MANUSCRIPT RECEIVED MARCH 16, 2005
MANUSCRIPT ACCEPTED OCTOBER 11, 2005
MANUSCRIPT HANDLED BY ALESSANDRO GUALTIERI